Proceedings of the
International Conference on Mechanical Engineering 2011
(ICME2011) 18-20 December 2011, Dhaka, Bangladesh

ICME11-FL-005

NUMERICAL STUDY OF A VISCOUS FLUID FLOW PAST A CIRCULAR CYLINDER IN AN UNBOUNDED DOMAIN.

A. K. Singha

Department of Jute and Fibre Technology, University of Calcutta,India

ABSTRACT

This paper describes a numerical study on heat transfer and fluid flow for unsteady, incompressible, Newtonian fluid past a circular cylinder in an unbounded domain based on Thompson, Thames, Mastin (TTM) method of automatic boundary fitted co-ordinate generation system. Finite difference implicit method, based on vorticity-stream function formulation with uniform inlet flow conditions, is employed for unsteady state computations for Reynolds numbers in the range 20-200. Length of recirculation zone and separation angle measured and the results are validated with previous work. Time-dependent periodic behavior of stream lines for Reynolds number from 50 up to 200 shows periodicity of flow field. The unsteady periodic shedding regime of vorticity isolines for Reynolds numbers are shown. The anti-clockwise positive vortices shed from the lower side of the cylinder and occupy the lower portion of the street. The clockwise negative vortices shed from upper side of the cylinder and occupy the upper portion of the street. The time-evolution of Nusselt number, averaged over the surface of the cylinder, for different Reynolds numbers are shown. The frequency of vortex shedding and the amplitude of the fluctuating average Nusselt number increases with Reynolds number.

Keywords: Unbounded Domain, Vorticity, Stream Function, Circular Cylinder, Finite Difference Method.

1. INTRODUCTION

The uniform flow past a circular cylinder in an unbounded domain has been investigated by many researchers both experimentally and numerically due to the practical importance of the flow. The flow in this type is characterized by the cylinder diameter (D), the free stream velocity (U) and the Reynolds number (Re). For flow past a circular cylinder, the separation of boundary layer on the cylinder surface begins at Reynolds number equal to 5 [1]. A pair of steady symmetric vortices develops behind the cylinder between Reynolds numbers 10 to 40 and the length of re-circulation zone grows linearly with increase in Reynolds number [2]. It is established that vortex shedding occurs for Reynolds number above 49. The vortex shedding flow remains laminar for Reynolds number up to around 150 [2]. Transition to three dimensional flow starts at Reynolds number of around 180-194, depending on experimental condition and ends at Reynolds number equal to about 260 at which fine scale three dimensional eddies appear [3]. The vortex shedding is regular and the Strouhal number, which represents vortex shedding frequency, remains unchanged. In Reynolds number from 300 to 1.4 x 10^5,the flow is in the sub-critical regime and the boundary layer along with the surface of the cylinder remains laminar throughout the circumference until flow separation takes place[4]. The vortex shedding is regular and the Strauhal number, which represents vortex shedding frequency, remains unchanged.

In the Reynolds number 5 to 40, Coutanceau and Bouard [5] measured the separation point and the length of the recirculation zone for single cylinder. They also measured the initial time evolution of the separation point and the formation length for an impulsively started cylinder[6]. Braza *et al*.[7] presented the time evaluation of the front stagnation point of a circular cylinder for Reynolds number up to 1000 based on finite volume solution to the Navier-Stokes equations. Karniadakis *et al*.[8] investigated forced convection heat transfer from an isolated cylinder in cross flow for Reynolds numbers up to 200 by direct numerical solution. In their paper they presented spatial structure of von Karman vortex street, the unsteady lift and drag co-efficient and unsteady local heat transfer co-efficient. They compared their results with available experimental data and found good agreement with it. D'Alessio and Dennis [9] have also developed a vorticity based technique to study the flow past a circular cylinder in an unconfined domain. The results are consistent with the boundary-layer flow approximation for sufficiently large values of the Reynolds number and with the asymptotic solution

obtained for low Reynolds number, at large distance from the cylinder. The authors also computed the various flow parameters for Reynolds number up to 100. Ding et *al*. [10] describe an efficient method for simulating two-dimensional steady and unsteady incompressible flow through a hybrid approach which combines the conventional finite difference scheme and mesh-less least square based finite difference method. They claimed that the new approach greatly improves the computational efficiency.

In this study, the two dimensional Navier-Stokes equations for time-dependent, viscous, incompressible flow along with continuity and energy equation are solved using vorticity-stream function formulation by finite difference method. The numerical method developed in this study is verificated against the benchmark problem of uniform flow past an unbounded circular cylinder. With this numerical procedure, the vortex shedding, vorticity isolines as well as heat transfer aspects across a circular cylinder in an unbounded domain are investigated.

2. MATHEMATICAL FORMULATION AND NUMERICAL SCHEME

In Cartesian co-ordinate systems, the non-dimensional governing equations, expressed in terms of vorticity and stream function, are written as,

$$\omega_t + (\mathbf{u}.\nabla)\omega = \frac{1}{\mathrm{Re}}\nabla^2\omega \qquad (1)$$

$$\nabla^2\psi = -\omega \qquad (2)$$

where ω represents vorticity, ψ denotes stream function, and $\mathbf{u} = (u, v)$, denote the components of velocity, which can be calculated from the stream function:

$$u = \partial_y\psi, \quad v = -\partial_x\psi \qquad (3)$$

The energy equation is expressed as:

$$\theta_t + (\mathbf{u}.\nabla)\theta = \frac{1}{\mathrm{Re}.\mathrm{Pr}}\nabla^2\theta \qquad (4)$$

In order to solve equations (1), (2), (3) and (4) in a curvilinear co-ordinate system, the following co-ordinate transformations are used:

$$\xi = \xi(x, y), \qquad \eta = \eta(x, y) \qquad (5)$$

in which (ξ, η) is the co-ordinate system in the computational plane. With the above transformation, the non-dimensional equations (1), (2), (3), and (4) are transformed into the computational co-ordinates (ξ, η) and written as:

$$\alpha\omega_{\xi\xi} + 2\beta\omega_{\xi\eta} + \gamma\omega_{\eta\eta} + \delta\omega_\xi + \varepsilon\omega_\eta = \mathrm{Re}[u(\omega_\xi\xi_x + \omega_\eta\eta_x) + v(\omega_\xi\xi_y + \omega_\eta\eta_y)] + \mathrm{Re}\,\omega_t \qquad (6)$$

$$\alpha\psi_{\xi\xi} + 2\beta\psi_{\xi\eta} + \gamma\psi_{\eta\eta} + \delta\psi_\xi + \varepsilon\psi_\eta = -\omega \qquad (7)$$

$$u = \xi_y\psi_\xi + \eta_y\psi_\eta \quad , \quad v = -(\xi_x\psi_\xi + \eta_x\psi_\eta) \qquad (8)$$

$$\alpha\theta_{\xi\xi} + 2\beta\theta_{\xi\eta} + \gamma\theta_{\eta\eta} + \delta\theta_\xi + \varepsilon\theta_\eta = \mathrm{Re}\,\mathrm{Pr}[u(\theta_\xi\xi_x + \theta_\eta\eta_x) + v(\theta_\xi\xi_y + \theta_\eta\eta_y)] + \mathrm{Re}\,\mathrm{Pr}\,\theta_t \qquad (9)$$

where, subscripts denote differentiation and coefficients are given by

$$\alpha = \xi_x^2 + \xi_y^2 \ , \ \beta = \xi_x\eta_x + \xi_y\eta_y \ , \ \gamma = \eta_x^2 + \eta_y^2 \ ,$$
$$\delta = \xi_{xx} + \xi_{yy}, \quad \varepsilon = \eta_{xx} + \eta_{yy} \qquad (10)$$

The solution of these transformed equations in the computational plane for unsteady flow starts with known uniform velocity and temperature field at inlet and always constrained by the boundary conditions.

3. PHYSICAL FLOW FIELD AND NUMERICAL PARAMETERS

A rectangular flow field is considered in this study as shown in Fig.1. The cylinder is considered at a distance of 5D from the inlet boundary and bottom boundary. The upper boundary of the computational domain is set at a distance of 10D from bottom wall and outlet boundary is set at 25D distance from cylinder center.

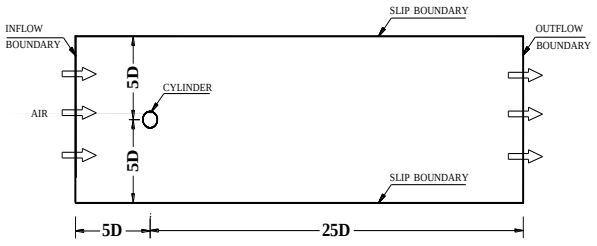

Fig 1. Configuration and boundary conditions of the flow

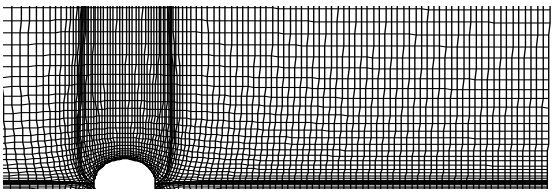

Fig 2. Mesh at upper half of the flow field.

Thompson, Thames, Mastin (TTM) method of generation of automatic boundary fitted co-ordinate generation system is used to construct the grids of the physical flow field. In this study, finite difference implicit method is used to solve the transformed governing equations.

A typical mesh arrangement (244 x 90) of complete flow field is considered. By (244 x 90) mesh, it is implied that there are 244 nodes in the longitudinal and 90 nodes in the transverse direction, respectively, with 72 nodes on cylinder surface. The mesh at upper half of the cylinder is shown in Fig. 2.

In this study, calculations are performed with a non-dimensional time step of t = 0.002. Care was taken in

refining the grid around the cylinder so that the smaller size of grid is around 0.002 to satisfy the convective stability condition and the diffusive accuracy.

4. BOUNDARY CONDITIONS

At inlet, uniform longitudinal velocity and zero transverse velocity is considered. No-slip boundary conditions are imposed on the cylinder surface. Boundary conditions for vorticity and stream function are described as follows:

The no slip boundary conditions for vorticity at cylinder surface can be written as per Thom's formula [11],

$$\omega_{ic,jc} = \frac{2(\psi_{ic,jc} - \psi_{ic,jc-1})}{h^2_{ic,jc}} \text{ at cylinder surface} \quad (11)$$

where (ic, jc) denotes the nodes on the cylinder surface and $h_{ic,jc}$ is the radial distance between cylinder surface and first body fitted node around the cylinder.

4.1 Boundary Condition for Stream Function at Cylinder Surface:

The no penetration boundary condition for u indicates that at cylinder surface

$$\psi = \text{constant} \quad (12)$$

while no-slip boundary condition for u at cylinder surface shows that

$$\frac{\partial \psi}{\partial n} = 0 \quad \text{and} \quad \int_{cyl} \frac{\partial \omega}{\partial n} = 0 \quad (13)$$

the value of ψ cyl is constant , which is updated for unsteady flow at every time step.

5. NUSSELT NUMBER

The local Nusselt number and average Nusselt number around the cylinder are determined by the following expression:

$$\text{Local Nusselt number : } Nu = \left(\frac{\partial \theta}{\partial R}\right)_{(R,\bar{\theta})} \quad (14)$$

$$\text{Average Nusselt number : } Nu_m = \frac{1}{2\pi}\int_0^{2\pi} Nu\, d\bar{\theta} \quad (15)$$

The local Nusselt number varies with angle around the cylinder. The angle, $\bar{\theta}$ is measured clockwise from the forward stagnation point.

6. RESULTS AND DISCUSSIONS

From the governing equations it is seen that the heat transfer and fluid flow characteristics depends upon Reynolds number and Prandtl number. In this paper the fluid is considered to be air with a Prandtl number of 0.705. In the following section, discussion is carried out on the transient aspects of the flow past the cylinder in an unbounded domain.

6.1 Recirculation Zone and Separation Angle

It is well known that the flow pattern changes with the Reynolds number. For Reynolds number up to approximately 49, the flow maintains a stable pattern with an attached pair of symmetrical vortices behind the cylinder. Numerical simulation is carried out for three small Reynolds numbers of 10, 20 and 40, respectively and the streamline patterns for these three Reynolds numbers are depicted in Fig. 4. In all cases, a pair of steady symmetric vortices develops behind the cylinder and is aligned symmetrically. These results are in good agreement with other researchers [12, 13] in terms of the flow parameters such as length of the recirculation zone, L_{sep}, and separation angle, θ_{sep} measured from the rear stagnation point of the cylinder to the end of the re-circulating region (Fig. 3) as presented in Table 1.

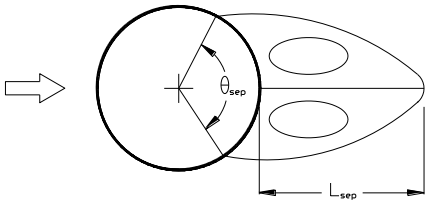

Fig 3. Definition re-circulation zone length (Lsep) and separation angle (θsep)

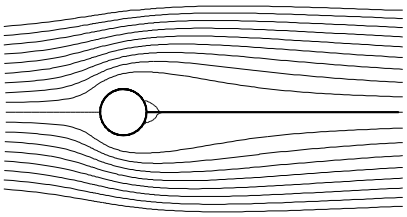

(a)

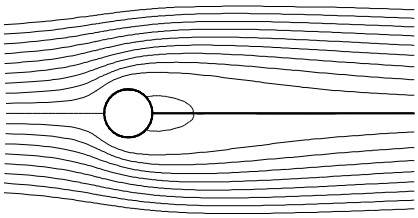

(b)

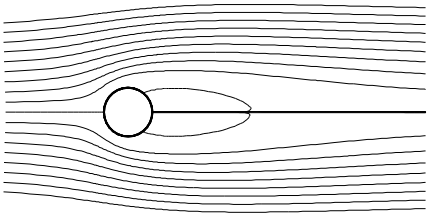

(c)

Fig 4. Streamlines for an unbounded cylinder: (a) Re = 10, (b) Re = 20 and (c) Re = 40.

Table 1: Comparison of re circulation zone length (L_{sep}) and separation angle (θ_{sep}) for Re = 10, 20 and 40.

Re		Dennis *et al.* [12]	Takami *et al.* [13]	Present
10	L_{sep}	0.252	0.249	0.26
	θ_{sep}	29.6	29.3	30.0
20	L_{sep}	0.94	0.935	0.90
	θ_{sep}	43.7	43.7	43
40	L_{sep}	2.35	2.32	2.08
	θ_{sep}	53.8	53.6	52

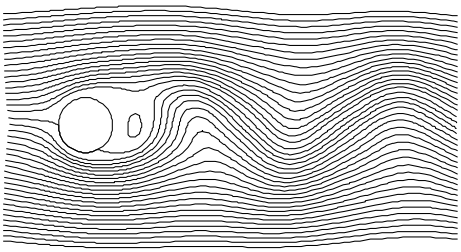

t=0

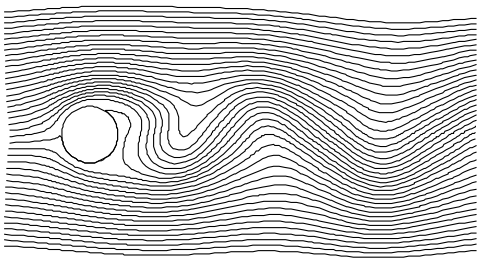

t = τ/3

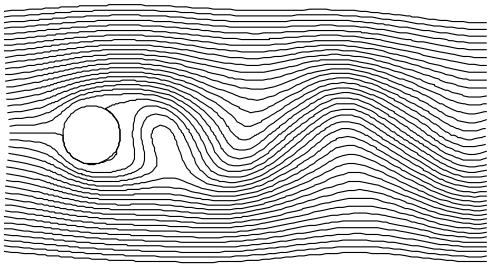

t = 2τ/3

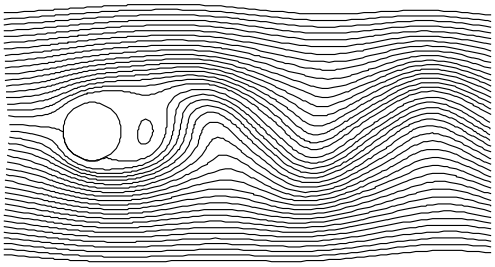

t = 3τ/3

Fig 5. The vortex shedding from an unbounded cylinder in a time cycle for Re = 100.

6.2 Vortex Shedding

At moderate Reynolds number, greater than approximately 49 and up to 150, the flow still remains laminar. Due to instability of shear layers on the wake of the cylinder, two- dimensional vortex shedding leads to the formation of von Karman vortex street; however, the flow is unsteady now. At a Reynolds number of 100, typical streamline patterns of the unsteady flow past an unbounded cylinder in a cross flow for a complete time cycle, of period τ is shown in Fig. 5, which are in good agreement with Karniadakis [8]. It is clear that periodicity of flow field is maintained in the Figure.

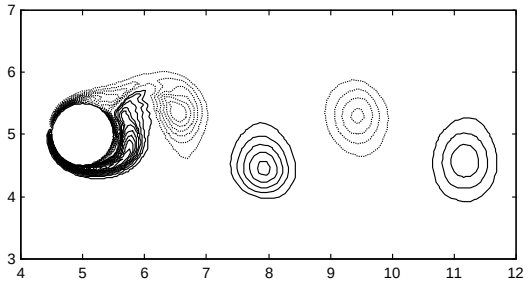

t=0

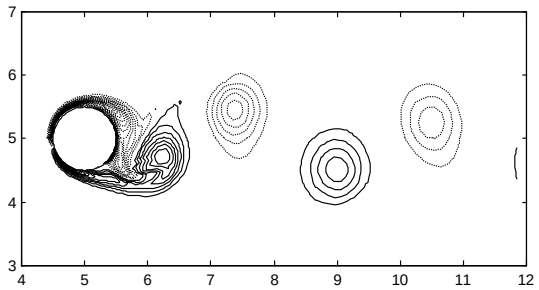

t = τ/3

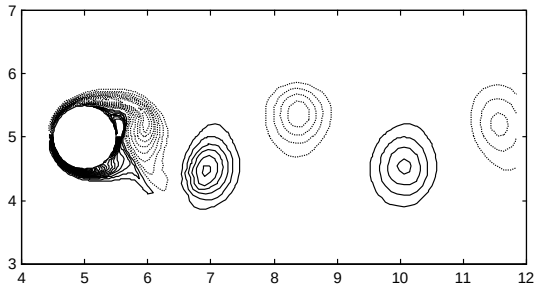

t = 2τ/3

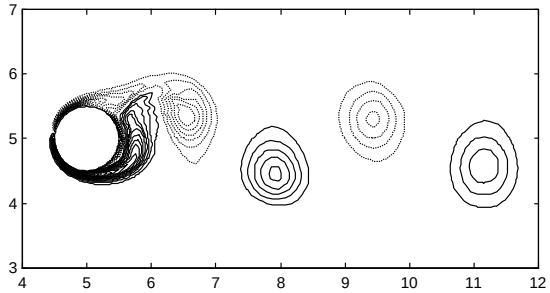

t = 3τ/3

Fig 6. The vorticity contours from an unbounded cylinder in a time cycle for Re = 200**.**

6.3 Vorticity Isolines

Fig. 6 shows the unsteady periodic shedding regime of vorticity isolines for Reynolds numbers of 200 over one time period. The positive (solid lines) and negative (dotted lines) vorticity contours are shown in the plot. As can be seen, the structure of vorticity field for the Reynolds numbers 200 is analogous to the classic von Karman vortex street. The clockwise negative vortices shed from upper side of the cylinder and they occupy the upper portion of the street. The anti-clockwise positive vortices shed from the lower side of the cylinder and they occupy the lower portion of the street.

6.4 Time Evolution of Average Nusselt Number

The time-evolution of Nusselt number, averaged over the surface of an unbounded cylinder, for different Reynolds numbers are shown in Fig. 7. As expected, at Reynolds number 40, no oscillations are observed as the flow remains steady and no vortex shedding takes place. Regularity of oscillations, as shown, for Reynolds

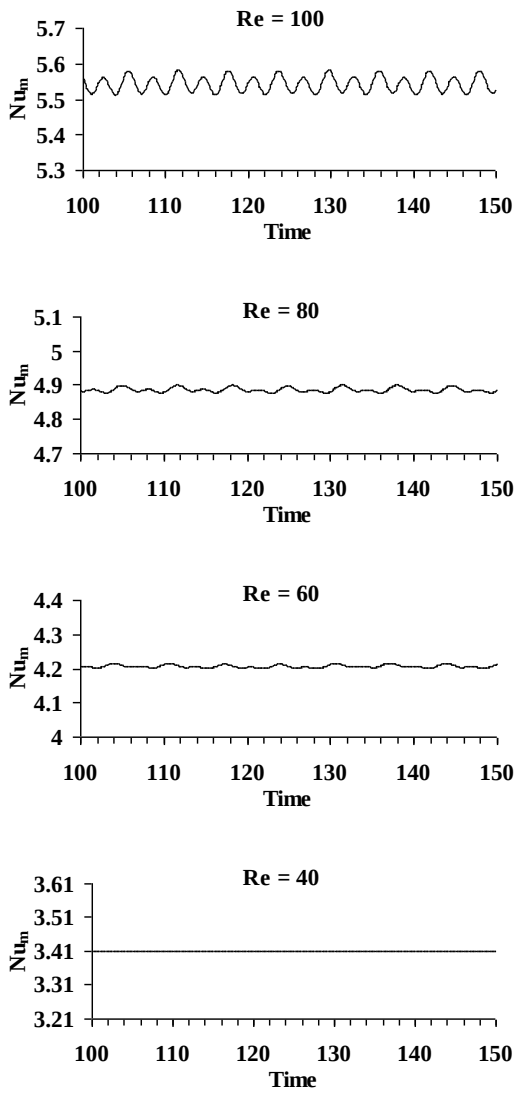

Fig 7. Time-evolution of the average Nusselt number for an unbounded cylinder for different Reynolds numbers

number higher than 40 indicates shedding of vortices at regular time interval. It is also evident from Fig. 7 that as the frequency of vortex shedding increases, the amplitude of the fluctuating average Nusselt number also increases with Reynolds number. Time-evolution of average Nusselt number for Reynolds number Re = 100, 80 and 60 also confirm this observation. The periodic rise and fall of average Nusselt number, as shown in Fig. 7, over a period of each shedding cycle is the consequence of development (formation and growth) and subsequent detachment of the pair of vortices in a cyclic manner at the wake of the cylinder. It is to be noted that there exists strong dissimilarity as far as the pattern of variation of average Nusselt number in each time cycle is concerned. This can be explained by the formation -growth-detachment cycle of vortices at the wake and its effect on heat transfer at the surface of the cylinder. For example, the formation and gradual growth of an eddy on either side of the cylinder may be assumed to be responsible for pushing off the main flow away from the cylinder surface. This is characterized by the sharp fall in the Nusselt number. On the contrary, detachment of an eddy, after the attainment of the critical size, is associated with splashing of the cylinder surface by the fresh fluid from mainstream and this results in a sharp increase in average Nusselt number. So it is seen that in a shedding cycle, for each of the two eddies, the Nusselt number initially decreases and then subsequently increases. Therefore, in a complete shedding cycle, starting from the growth to the detachment of eddies on either side of the cylinder, there have two time intervals when Nusselt number increases and in the other two intervals, Nusselt number decreases. This explanation is in confirmation to the pattern of variation of the Nusselt number as shown in Fig. 7.

7. CONCLUSION

In this numerical study, heat transfer for non-isothermal flow past a circular cylinder in an unbounded domain is considered. An implicit finite difference method is used and solution to the two-dimensional Navier-Stokes equation and Energy equation for laminar unsteady incompressible viscous flows has been obtained. The flow is calculated for Reynolds Numbers range from 20 to 200 . Based on the numerical solutions, effect of Reynolds Numbers on fluid parameters are investigated.

The major findings are summarized below.

a. At low Renolds number up to 40, a pair of steady symmetric vortices develops behind the cylinder and is aligned symmetrically. Re circulation zone length and separation angle increases with Renolds number.

b. At higher Renolds number, in the vortex shedding regime, the clockwise negative vortices shed from upper side of the cylinder and they occupy the upper portion of the street. The anti-clockwise positive vortices shed from the lower side of the cylinder and they occupy the lower portion of the street.

c. As the Reynolds number increases, the frequency of vortex shedding increases as seen from the Time – evolution of the average Nusselt number, the amplitude of the fluctuating average Nusselt number also increases.

d. The periodic rise and fall of average Nusselt number on the time-evolution of Nusselt number, over each of shedding cycle is the consequence of development (formation and growth) and subsequent detachment of the pair of vortices in a cyclic manner at the wake of the cylinder.

6. REFERENCES

1. Taneda, S., 1965, "Experimental investigation of the wakes behind cylinders and plates at low Reynolds numbers", Journal of Physical Society of Japan, 11: 302-965.
2. Beaudan, P., Moin, P., 1994, "Numerical Experiments on the flow past a circular cylinder at sub-critical Reynolds number", Report no TF-62, Department of Mechanical Engineering, Standford University, Standford, California, USA.
3. Williamson, C. H. K., 1996, "Vortex dynamics in the cylinder wake", Annual review of Fluid Mechanics, 28: 477-539.
4. Niemann, H.J., Holscher, N., 1990 "A review of recent experiments on the flow Past circular cylinders", Journal of Wind Engineering and Industrial aerodynamics, 33: 197-209.
5. Coutanceau, M., Bouard, R., 1977, "Experimental determination of main features of Viscous flow in the wake of a circular cylinder in uniform translation", Part – I, Unsteady flow, Journal of Fluid Mechanics, 79(2): 231-256.
6. Coutanceau, M., Bouard, R., 1977, "Experimental determination of main features of Viscous flow in the wake of a circular cylinder in uniform translation", Part – II, Unsteady flow. Journal of Fluid Mechanics, 79(2): 257-272.
7. Braza, M., Chassaing, P., Ha Minh, H., 1986, "Numerical Study and physical Analysis of the pressure and velocity fields in the near wake of a circular Cylinder", Journal of Fluid Mechanics, 165: 79-130.
8. Karniadakis, George EM., 1988 "Numerical simulation of forced convection heat transfer from a cylinder in crossflow", Journal of Heat and Mass Transfer, 31: 107-118.
9. Alessio, S.J.D.D, Dennis, S.C.R., 1994, "A vorticity model for viscous flow past a cylinder", Computers & Fluids, 23: 279-293.
10. Ding, H., Shu, C., Yeo, K.S. Xu, D., 2004, "Simulation of incompressible viscous flow past a circular cylinder by hybrid FD scheme and mesh-less least square–based finite difference method", Computer Methods of Applied Mechanics Engineering, 193: 727-744.
11. Thom, A., 1933, "The flow past circular cylinders at low speeds", Proc R Soc London Sect A, 141: 651-669.
12. Dennis, S. C. R., Chang, G.Z., 1970, "Numerical solutions for steady flow past a circular cylinder at Reynolds number up to 100", Journal of Fluid Mechanics, 42: 471.
13. Takami, H., Keller, H.B., 1969, "Steady two-dimensional viscous flow of an incompressible fluid past a circular cylinder", Physics of Fluids, 12 (Suppl.II): II-51.

7. MAILING ADDRESS

Dr. A. K. Singha
Associate Professor in Mechanical Engineering
Department of Jute and Fibre Technology
University of Calcutta
35 Ballygunge Circular Road
Kolkata-700019
WB, India.
Phone : +91 33 2461 5444
FAX : +91 33 2461 5632.
E-mail : amiya_singha@rediffmail.com